Available online at www.sciencedirect.com

SCIENCE DIRECT®

ELSEVIER

International Journal of Mass Spectrometry 247 (2005) 101–105

International Journal of Mass Spectrometry

www.elsevier.com/locate/ijms

Site-specific fragmentation caused by core-level photoexcitation: Comparison between Si:1s and 2p photoexcitations in $F_3SiCH_2CH_2Si(CH_3)_3$ vapor

Shin-ichi Nagaoka[a,∗], Asuka Tamura[a], Akiko Fujii[a], Joji Ohshita[b], Kazumasa Okada[c], Toshio Ibuki[d], Isao H. Suzuki[e], Haruhiko Ohashi[f], Yusuke Tamenori[f]

[a] *Department of Chemistry, Faculty of Science, Ehime University, Matsuyama 790-8577, Japan*
[b] *Department of Applied Chemistry, Faculty of Engineering, Hiroshima University, Higashi-Hiroshima 739-8527, Japan*
[c] *Department of Chemistry, Faculty of Science, Hiroshima University, Higashi-Hiroshima 739-8526, Japan*
[d] *Kyoto University of Education, Fushimi-ku, Kyoto 612-8522, Japan*
[e] *National Institute of Advanced Industrial Science and Technology (AIST), Tsukuba 305-8568, Japan*
[f] *Japan Synchrotron Radiation Research Institute (JASRI), 1-1-1 Kouto, Mikazuki-cho, Sayo-gun, Hyogo 679-5198, Japan*

Received 20 July 2005; received in revised form 6 October 2005; accepted 6 October 2005
Available online 16 November 2005

Abstract

Ionic fragmentation caused by Si:1s photoexcitation of 1-trifluorosilyl-2-trimethylsilylethane [$F_3SiCH_2CH_2Si(CH_3)_3$] vapor was studied using monochromatized synchrotron radiation and a reflectron-type mass spectrometer. The total ion-yield spectrum in the Si:1s excitation region was found to be very similar to the superposition of the ion-yield spectra of $Si(CH_3)_4$ and SiF_4, showing that site-specific excitation occurred in this molecule. When the photon energy was scanned from low to high, the $1s \rightarrow \sigma^*$ excitation at the Si atom bonded to three CH_3 groups suppressed the production of CH_3^+ and $SiCH_3^+$. The $1s \rightarrow \sigma^*$ excitation at the Si atom bonded to three F atoms, on the other hand, enhanced the production of F^+ and SiF^+ and suppressed the production of SiF_3^+. These results suggest that Si:1s site-specific excitation causes site-specific fragmentation. The fragmentation caused by Si:1s $\rightarrow \sigma^*$ photoexcitation was also found to be more violent than that caused by Si:2p $\rightarrow \sigma^*$ photoexcitation.

Keywords: Site-specific fragmentation; Core-level photoexcitation; Organosilicon molecule; Synchrotron radiation

---

1. Introduction

A core electron of an atom in a molecule is localized very close to the nucleus, and the excitation energy required by a core electron depends on the chemical environment of the atomic site. Monochromatized synchrotron radiation can excite core electrons of an atom in a specific chemical environment selectively, discriminating them from those of like atoms in different chemical environments. This site-specific excitation often results in site-specific fragmentation [1–7], which is potentially useful for controlling chemical reactions by dissociating bonds selectively. Site-specific fragmentation also offers possibilities of analyzing the structures and properties of molecules, molecular assemblies and nanoscale devices by controlling matter at the level of individual atoms. To realize these possibilities we need to understand what controls behavior at the atomic level.

1-Trifluorosilyl-2-trimethylsilylethane [$F_3SiCH_2CH_2Si(CH_3)_3$, FSMSE] is a promising molecule for the study of site-specific excitation and fragmentation because the chemical environment of a silicon atom bonded to three fluorine atoms (here denoted Si[F]) is very different from that of one bonded to three methyl groups (Si[Me]) [8–10]. The dimethylene group ($–CH_2CH_2–$) between the two Si atoms impairs intersite electron migration and protects site-specificity in the fragmentation [11,12]. In this molecule, it is very interesting to compare the ionic fragmentation due to the photoexcitation of Si:1s electrons with that due to the photoexcitation of Si:2p electrons: Photoexcitation from the Si:1s orbital to an antibonding orbital (σ^*) often leads to multistep Auger transitions and the formation of a multiply charged parent-ion. The resultant decomposition

---

∗ Corresponding author. Fax: +81 89 927 9590.
E-mail address: nagaoka@ehimegw.dpc.ehime-u.ac.jp (S. Nagaoka).

1387-3806/$ – see front matter © 2005 Elsevier B.V. All rights reserved.
doi:10.1016/j.ijms.2005.10.003

due to Coulombic repulsion among these multiple charges is expected to be more violent than the decomposition caused by Si:2p → σ^* photoexcitation, which leads to single-step Auger transitions.

The site-specific fragmentation caused by Si:1s → σ^* photoexcitation in organosilicon molecules, however, has not yet been studied because it has been hard to obtain, with high resolution, the 1850 eV photons needed for exciting Si:1s electrons. Conventional grazing-incidence grating monochromators with high resolution were usually used for experiments with electron energies up to ≅1 keV, and double-crystal monochromators were utilized for those with electron energies above 2 keV. It was thus difficult to make practical use of monochromatized synchrotron radiation with high resolution in the region of 1–2 keV. Although monochromatized output in the Si:1s edge region has been obtained by installing InSb(1 1 1) single crystals in double-crystal monochromators [13,14], there is some question as to their heat-resistance.

Recent developments in optics components, as well as the recent construction of third-generation synchrotron radiation facilities, have made it possible to perform various experiments in the above-mentioned intermediate photon energy range. We have used monochromatized output in the intermediate range to study relaxation processes caused by Kr:2p photoexcitation (≈1700 eV) [15–17], which cannot be attained from a double-crystal monochromator equipped with InSb(1 1 1) single crystals. The present paper reports the site dependence of ion yields in the Si:1s → σ^* photoexcitation of FSMSE and compares it with that of ion yields in Si:2p → σ^* photoexcitation.

2. Experimental

FSMSE was synthesized from CuF_2 and 1-trichlorosilyl-2-trimethylsilylethane prepared from trimethylvinylsilane, trichlorosilane and 1.0 M $H_2PtCl_6 \cdot 6H_2O$/isopropyl alcohol [8].

The experiments were performed using the high-resolution plane-grating monochromator installed in the c branch of the soft X-ray figure-8 undulator beamline 27SU at the SPring-8 facility [18,19]. The beamline provided linearly polarized monochromatized synchrotron radiation (0.17–3 keV) with a resolution $E/\Delta E$ better than 5400 at $E = 1.5$ keV. The available photon flux was 1×10^{11} photons/s/100mA/0.02%-bandwidth at 2 keV, and at the sample position the beam was about 0.2 mm in diameter. A large monochromator slit-width ($E/\Delta E = 3500$) was used to obtain sufficient signal intensity within a reasonable accumulation time. The energy and resolution of the monochromatized photons (E and $E/\Delta E$, respectively) were calibrated by using the Kr:$2p_{3/2}$ photoelectron peak (binding energy: 1678.4 eV [20]) measured with a hemispherical electron-energy analyzer (GAMMADATA SES-2002) that had been calibrated against the energy of Kr:$L_3M_{45}M_{45}$ $^1G_4$ normal-Auger peak (1460.1 eV [21]). The intensity of the monochromatized photon beam (I_{photon}) was monitored by measuring the drain current of the post-focusing mirror at the beamline, and the spectral sensitivity of the drain current was assumed to be constant within the photon energy region of interest.

After the main chamber was evacuated to a pressure below 10^{-6} Pa, sample gas was introduced through a 1/16-in. needle until the pressure in which was 3×10^{-4} Pa. The experiments were performed using a variable-angle reflectron time-of-flight (TOF) mass spectrometer [18,22,23]. The axis of the TOF tube, the incident monochromatized photon beam and the sample-gas beam were mutually perpendicular. The axis of the TOF tube made an angle of 55° with respect to the electric vector of the linearly polarized synchrotron radiation. The electrons and ions were extracted in opposite directions with a static electric field of 72 V/mm applied across the ionization region during the measurement. With the aid of the mass spectrometer, the total ion intensity ($I_{\mathrm{tot\text{-}ion}}$) was detected with a Microsphere Plate (MSP; El-Mul C033DTA). Photoionization mass spectra were obtained by feeding the signals from the electron detector (MSP; El-Mul C033DTA) into the start pulse input of a single-hit time-to-amplitude converter (TAC) and feeding the signals from the TOF mass spectrometer into the stop pulse input of the TAC. The dwell time of the TAC was 25 ns/channel. The output signals from the TAC were sent to a multichannel analyzer (MCA) unit in a personal computer that processed these signals into a TOF mass spectrum.

3. Results and discussion

3.1. Si:1s photoexcitation

Fig. 1A shows the total ion-yield spectrum ($I_{\mathrm{tot\text{-}ion}}/I_{\mathrm{photon}}$) near the Si:1s ionization threshold of FSMSE vapor. One can see three sharp peaks and one broad peak in the spectrum, which approximates the photoabsorption cross-section on a relative

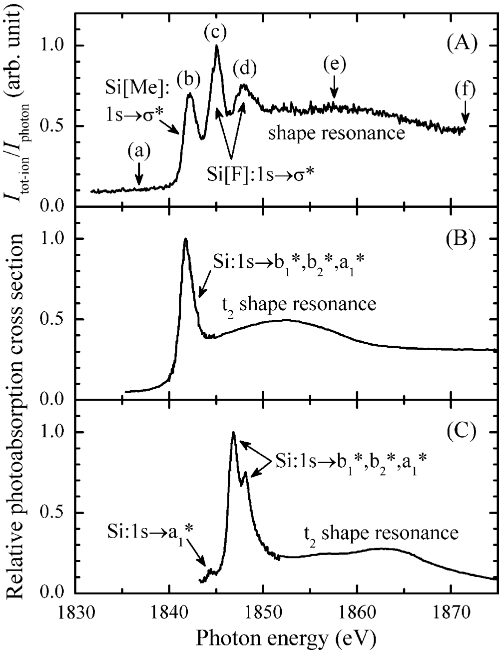

Fig. 1. (A) $I_{\mathrm{tot\text{-}ion}}/I_{\mathrm{photon}}$ near the Si:1s ionization threshold of FSMSE vapor. The letters (a–f) indicate the photon energies used in the measurements of the individual spectra shown in Fig. 2. Photoabsorption spectrum of: (B) $Si(CH_3)_4$ vapor [24] and (C) SiF_4 vapor [24].

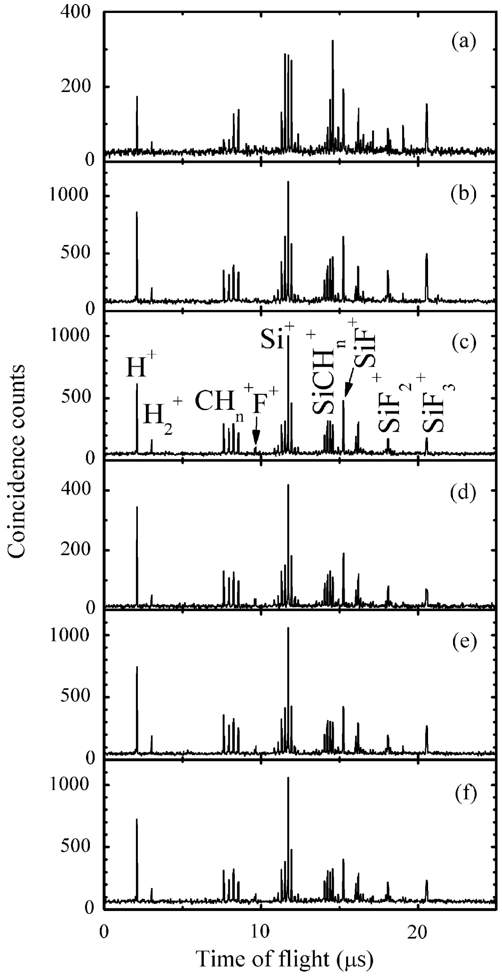

Fig. 2. FSMSE vapor photoionization mass spectra obtained at the photon energies indicated by (a–f) in Fig. 1A. Data collection times for each data point were: (a) 18351 s, (b) 9045 s, (c) 4440 s and (d–f) 7200 s.

scale. The peak assignments inferred by comparison with the photoabsorption spectra of $Si(CH_3)_4$ and SiF_4 vapors (Fig. 1B and C [24]) are indicated in Fig. 1A. The $I_{\text{tot-ion}}/I_{\text{photon}}$ spectrum of FSMSE is very similar to the superposition of the photoabsorption spectra of $Si(CH_3)_4$ and SiF_4, showing that site-specific excitation indeed occurs in FSMSE.

Parts (a–f) of Fig. 2, respectively, show the photoionization mass spectra of FSMSE vapor that were obtained at the photon energies indicated by (a–f) in Fig. 1A. For convenience, we divide the various ions seen in the spectra into groups A–C. The group A ions – CH_3^+, $SiCH_3^+$, $Si(CH_3)_2^+$ and $Si(CH_3)_3^+$ – are produced through dissociations of only the Si–C bonds surrounding the Si[Me] site, whereas the group B ions – F^+, SiF^+, SiF_2^+ and SiF_3^+ – are produced through dissociations of only the Si–F and Si–C bonds surrounding the Si[F] site. The group C ions are produced through the dissociations of several bonds in the vicinity of either the Si[Me] site, the Si[F] site or both sites. Although rearrangement (isomerization) is not extensive in direct fragmentations from organosilicon parent-ions [25], some rearrangement ions seen in the mass spectra of FSMSE-related molecules [26] are classified into group C. However, the fragmentation related to group C ions is not treated in this paper.

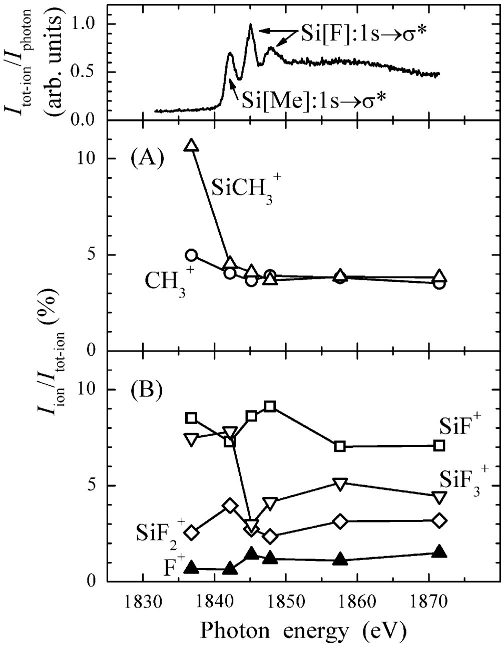

Fig. 3. (Top panel) Plot of $I_{\text{tot-ion}}/I_{\text{photon}}$ as a function of photon energy near the Si:1s ionization threshold of FSMSE vapor. Plots of $I_{\text{ion}}/I_{\text{tot-ion}}$ for: (A) group A ions and (B) group B ions.

Ratios of the integrated intensities of various ion peaks in the photoionization mass spectra to the total ion intensity ($I_{\text{ion}}/I_{\text{tot-ion}}$) are plotted against photon energy (near the Si:1s ionization threshold) in Fig. 3, which for comparison also shows the total ion-yield spectrum ($I_{\text{tot-ion}}/I_{\text{photon}}$). Fig. 3A and B are, respectively, the $I_{\text{ion}}/I_{\text{tot-ion}}$ plots for ions of groups A and B. The abundances of $Si(CH_3)_2^+$ and $Si(CH_3)_3^+$ (group A ions) are small.

As shown in Fig. 3B, the production of F^+ and SiF^+ ions is enhanced at the Si[F]:1s → σ^* photoexcitation energy. That is,

$$\text{Si[F]} : 1\text{s} \rightarrow \sigma^* \text{ excitation :}$$

$$F_3SiCH_2CH_2Si(CH_3)_3 \rightarrow F^+ \text{ and/or } SiF^+. \qquad (1)$$

Site-specific fragmentation caused by Si[F]:1s → σ^* photoexcitation is evident in FSMSE vapor. The enhanced production of F^+ and SiF^+ shows that Si[F]–F and Si[F]–C bonds must have been dissociated. Thus, the site-specific bond dissociation occurs at the Si[F] atom where the photoexcitation has taken place.

The production of SiF_3^+ ions is suppressed at the Si[F]:1s → σ^* photoexcitation energy even though the production of F^+ and SiF^+ ions is enhanced there (Fig. 3B). The extent of decomposition is thus enhanced by Si[F]:1s → σ^* photoexcitation. The SiF_3 group is destroyed by the Si[F]:1s → σ^* photoexcitation because the ionic fragmentation usually takes place in the vicinity of the core-excited Si[F] site. This is probably the reason that the production of SiF_3^+ ions is suppressed at the Si[F]:1s → σ^* resonance.

As shown in Fig. 3A, the production of CH_3^+ and $SiCH_3^+$ ions is suppressed at the Si[Me]:1s → σ^* photoexcitation energy, and the $I_{\text{ion}}/I_{\text{tot-ion}}$ values of these ions are nearly constant above the threshold of the Si[F]:1s photoexcitation. This suppression of

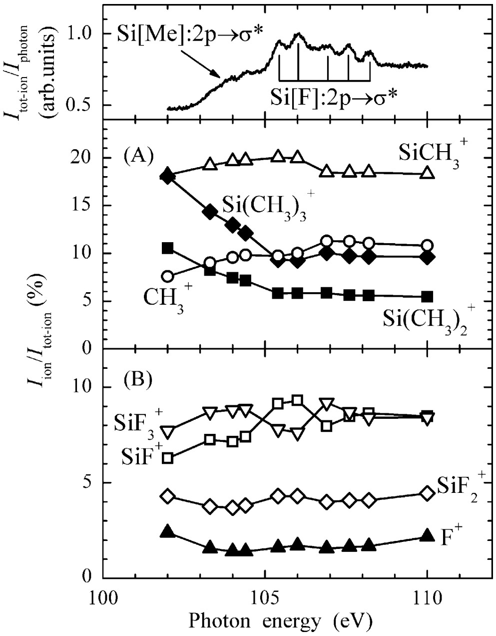

Fig. 4. (Top panel) Plot of $I_{tot-ion}/I_{photon}$ as a function of photon energy near the Si:2p ionization threshold of FSMSE vapor. Plots of $I_{ion}/I_{tot-ion}$ for: (A) group A ions and (B) group B ions. These results were obtained with an optical resolution of $E/\Delta E = 600$ at the BL3A2 beamline of the UVSOR facility [8].

CH_3^+ and $SiCH_3^+$ production is also likely due to the enhanced extent of decomposition caused by Si:1s → σ^* photoexcitation. Site-specific fragments formed through the Si[Me]:1s → σ^* photoexcitation may be the source of some group C ions. Thus,

Si[Me] : 1s → σ^* excitation :

$$F_3SiCH_2CH_2Si(CH_3)_3 \rightarrow \text{some group C ions.} \quad (2)$$

3.2. Comparison with Si:2p photoexcitation

A previous study [8] showed that site-specific fragmentation of FSMSE is also caused by Si:2p → σ^* photoexcitation in the vapor phase. The top panel of Fig. 4 shows $I_{tot-ion}/I_{photon}$ plotted as a function of photon energy near the Si:2p ionization threshold of FSMSE vapor. Peak assignments are given in that panel, and the $I_{ion}/I_{tot-ion}$ plots for groups A and B ions are shown in Fig. 4A and B.

Si[F]:2p → σ^* photoexcitation enhances the production of SiF^+ ions and suppresses the production of SiF_3^+ ions (Fig. 4B). Since the peak at 106.9 eV in the $I_{tot-ion}/I_{photon}$ plot for Si[F]:2p → σ^* excitation is lower than the other peaks in that plot, the $I_{ion}/I_{tot-ion}$ curve for SiF^+ drops at 106.9 eV and the $I_{ion}/I_{tot-ion}$ curve for SiF_3^+ rises there [12]. This means that

Si[F] : 2p → σ^* excitation :

$$F_3SiCH_2CH_2Si(CH_3)_3 \rightarrow SiF^+. \quad (3)$$

Si[F]:2p → σ^* photoexcitation and Si[F]:1s → σ^* photoexcitation both increase the extent of FSMSE decomposition, but the production of F^+ ions is negligibly increased by Si[F]:2p → σ^* photoexcitation (Fig. 4B), whereas it is clearly increased by Si[F]:1s → σ^* photoexcitation (Fig. 3B). Thus, the extent of FSMSE decomposition due to Si[F]:2p → σ^* is less than that due to Si[F]:1s → σ^* photoexcitation.

Abundant $Si(CH_3)_2^+$ and $Si(CH_3)_3^+$ (group A ions) are seen in the photoionization mass spectra obtained at the photon energies of Si:2p → σ^* excitation (Fig. 4A), in contrast to what is seen in the spectra obtained at the photon energies of Si:1s → σ^* excitation (Figs. 2 and 3). At the Si[Me]:2p → σ^* photoexcitation energies, the production of $Si(CH_3)_2^+$ and $Si(CH_3)_3^+$ ions is suppressed while that of $SiCH_3^+$, which is smaller than $Si(CH_3)_2^+$ and $Si(CH_3)_3^+$, is enhanced slightly. This means that

Si[Me] : 2p → σ^* excitation :

$$F_3SiCH_2CH_2Si(CH_3)_3 \rightarrow SiCH_3^+. \quad (4)$$

Thus, the extent of FSMSE decomposition is increased by Si[Me]:2p → σ^* photoexcitation as well as by Si[Me]:1s → σ^* photoexcitation. A difference, however, between the fragmentations due to the Si[Me]:2p → σ^* and Si[Me]:1s → σ^* photoexcitations should be noted. Si[Me]:2p → σ^* photoexcitation suppresses the production of $Si(CH_3)_2^+$ and $Si(CH_3)_3^+$ and slightly enhances the production of $SiCH_3^+$ (Fig. 4A), whereas Si[Me]:1s → σ^* photoexcitation suppresses the production of $SiCH_3^+$ (Fig. 3A). Thus, the extent of decomposition due to Si[Me]:2p → σ^* photoexcitation is less than due to Si[Me]:1s → σ^* photoexcitation.

As described above, although the extent of FSMSE decomposition is enhanced by Si:2p → σ^* photoexcitation, it is not enhanced as much as it is by Si:1s → σ^* photoexcitation. The result can be explained in terms of two facts. One is that, as noted in Section 1, Si:1s → σ^* photoexcitation leads to multistep Auger transitions, whereas Si:2p → σ^* photoexcitation leads to single-step Auger transitions. The other is that the initial energy deposition due to Si:1s → σ^* photoexcitation is larger than that due to Si:2p → σ^* photoexcitation.

4. Conclusions

The ionic fragmentation caused by the Si:1s → σ^* photoexcitation of FSMSE vapor was studied by using monochromatized synchrotron radiation and a reflectron-type mass spectrometer. The $I_{tot-ion}/I_{photon}$ and $I_{ion}/I_{tot-ion}$ spectra in the Si:1s excitation region suggested that site-specific excitation and fragmentation occurred in this molecule. When this fragmentation was compared with that caused by Si:2p → σ^* photoexcitation, the extent of decomposition due to Si:1s → σ^* photoexcitation was found to be larger than that of the decomposition due to Si:2p → σ^* photoexcitation.

Acknowledgements

We express our sincere thanks to the members of the SPring-8 research team for soft X-ray photochemistry for their fruitful discussions. Our thanks are also due to Mr. Shingo Samori of Kyoto University of Education and the members of the SPring-8 facility for their valuable help during the course of the experiments. S.N. and J.O. thank Professor Takae Takeuchi of Nara

Women's University for her valuable discussion on the rearrangement ions of FSMSE. This study was performed with the approval of JASRI as Nanotechnology Support Projects (Proposal Nos. 2002A0029-NS1-np, 2002B0101-NS1-np and 2003A0023-NS1-np) of the Ministry of Education, Culture, Sports, Science and Technology of Japan (MEXT). S.N. and I.H.S. are grateful for financial support provided by a Grant-in-Aid for Scientific Research from MEXT and by the Budget for Nuclear Research, respectively.

Appendix A. Supplementary data

Supplementary data associated with this article can be found, in the online version, at doi:10.1016/j.ijms.2005.10.003.

References

[1] W. Eberhardt, T.K. Sham, R. Carr, S. Krummacher, M. Strongin, S.L. Weng, D. Wesner, Phys. Rev. Lett. 50 (1983) 1038.
[2] K. Müller-Dethlefs, M. Sander, L.A. Chewter, E.W. Schlag, J. Phys. Chem. 88 (1984) 6098.
[3] D.M. Hanson, Adv. Chem. Phys. 77 (1990) 1.
[4] I. Nenner, C. Reynaud, H.C. Schmelz, L. Ferrand-Tanaka, M. Simon, P. Morin, Z. Phys. Chem. 195 (1996) 43.
[5] S. Nagaoka, K. Mase, I. Koyano, Trends Chem. Phys. 6 (1997) 1.
[6] R. Romberg, N. Heckmair, S.P. Frigo, A. Ogurtsov, D. Menzel, P. Feulner, Phys. Rev. Lett. 84 (2000) 374.
[7] K. Tanaka, E.O. Sako, E. Ikenaga, K. Isari, S.A. Sardar, S. Wada, T. Sekitani, K. Mase, N. Ueno, J. Electron Spectrosc. Relat. Phenom. 119 (2001) 255.
[8] S. Nagaoka, T. Fujibuchi, J. Ohshita, M. Ishikawa, I. Koyano, Int. J. Mass Spectrom. Ion Process. 171 (1997) 95.
[9] S. Nagaoka, K. Mase, M. Nagasono, S. Tanaka, T. Urisu, J. Ohshita, J. Chem. Phys. 107 (1997) 10751.
[10] S. Nagaoka, Y. Tamenori, M. Hino, T. Kakiuchi, J. Ohshita, K. Okada, T. Ibuki, I.H. Suzuki, Chem. Phys. Lett. 412 (2005) 459.
[11] S. Nagaoka, K. Mase, M. Nagasono, S. Tanaka, T. Urisu, J. Ohshita, U. Nagashima, Chem. Phys. 249 (1999) 15.
[12] S. Nagaoka, T. Fujibuchi, J. Ohshita, U. Nagashima, I. Koyano, Chem. Phys. 276 (2002) 243.
[13] K. Kitajima, Y. Takata, A. Toyoshima, H. Maezawa, Rev. Sci. Instrum. 63 (1992) 886, and references therein.
[14] B.X. Yang, F.H. Middleton, B.G. Olsson, G.M. Bancroft, J.M. Chen, T.K. Sham, K. Tan, D.J. Wallace, Rev. Sci. Instrum. 63 (1992) 1355, and references therein.
[15] S. Nagaoka, T. Ibuki, N. Saito, Y. Shimizu, Y. Senba, K. Kamimori, Y. Tamenori, H. Ohashi, I.H. Suzuki, J. Phys. B 33 (2000) L605.
[16] I.H. Suzuki, A. Fujii, S. Nagaoka, M. Kosugi, K. Okada, T. Ibuki, S. Samori, Y. Tamenori, H. Ohashi, J. Phys. B 37 (2004) 1433.
[17] K. Okada, M. Kosugi, A. Fujii, S. Nagaoka, T. Ibuki, S. Samori, Y. Tamenori, H. Ohashi, I.H. Suzuki, K. Ohno, J. Phys. B 38 (2005) 421.
[18] H. Ohashi, E. Ishiguro, Y. Tamenori, H. Kishimoto, M. Tanaka, M. Irie, T. Tanaka, T. Ishikawa, Nucl. Instrum. Methods A 467–468 (2001) 529.
[19] Y. Tamenori, H. Ohashi, E. Ishiguro, T. Ishikawa, Rev. Sci. Instrum. 73 (2002) 1588.
[20] K. Siegbahn, C. Nordling, G. Johansson, J. Hedman, P.F. Hedén, K. Hamrin, U. Gelius, T. Bergmark, L.O. Werme, R. Manne, Y. Baer, ESCA Applied to Free Molecules, North-Holland, Amsterdam, 1969, p. 41.
[21] J.C. Levin, S.L. Sorensen, B. Crasemann, M.H. Chen, G.S. Brown, Phys. Rev. A 33 (1986) 968.
[22] A. Hiraya, Y. Senba, H. Yoshida, K. Tanaka, J. Electron Spectrosc. Relat. Phenom. 101–103 (1999) 1025.
[23] I. Koyano, M. Okuyama, E. Ishiguro, A. Hiraya, H. Ohashi, T. Kanashima, K. Ueda, I.H. Suzuki, T. Ibuki, J. Synchrotron Radiat. 5 (1998) 545.
[24] S. Bodeur, I. Nenner, P. Millie, Phys. Rev. A 34 (1986) 2986.
[25] T. Takeuchi, M. Tanaka, T. Matsutani, M. Kiuchi, Surf. Coat. Technol. 158–159 (2002) 408.
[26] S. Nagaoka, J. Ohshita, M. Ishikawa, K. Takano, U. Nagashima, T. Takeuchi, I. Koyano, J. Chem. Phys. 102 (1995) 6078.